Available online at www.sciencedirect.com

ScienceDirect

Ceramics International 35 (2009) 2699–2704

CERAMICS INTERNATIONAL

www.elsevier.com/locate/ceramint

The growth of interfacial compounds between titanium dioxide and bismuth oxide

C.-D. Lu, L.-S. Chang *, Y.-F. Lu, F.-H. Lu

Department of Materials Science and Engineering, National Chung Hsing University, Taichung, Taiwan, ROC

Received 28 January 2009; received in revised form 4 February 2009; accepted 2 March 2009
Available online 27 March 2009

Abstract

The growth of interfacial compounds between TiO_2 and Bi_2O_3 during transient liquid phase bonding at 900, 1000 and 1100 °C for various times was investigated. The microstructures and compositions of compounds in joints were analyzed by means of SEM and EPMA. It was found that the compound $Bi_4Ti_3O_{12}$ forms initially and replaces the Bi_2O_3 interlayer. $Bi_2Ti_4O_{11}$ then arises at the interface between $Bi_4Ti_3O_{12}$ and TiO_2 and the metastable $Bi_2Ti_2O_7$ phase appears last at the interface between $Bi_4Ti_3O_{12}$ and $Bi_2Ti_4O_{11}$. The modes and activation energies of the growth of $Bi_4Ti_3O_{12}$ and $Bi_2Ti_4O_{11}$ were determined respectively. Holes in the middle of the joint heated at 1100 °C for 24 h were also found.

Keywords: A. Joining; B. Interfaces; B. Microstructure-final; D. TiO_2; Bi_2O_3

1. Introduction

The joining of industrial ceramic has been considered as a high-cost and time-consuming task. There are mainly two different ways: diffusion bonding and brazing. Ceramics joined by diffusion bonding usually has excellent strength and toughness; however, it takes a lot of time and energy. For example, the joining of alumina by diffusion bonding has been carried out at 1500 °C under a uniaxial pressure of 138 MPa and a post 3 h heat treatment at 1875 °C [1]. Comparably, brazing, especially active brazing, has a lower operating temperature and even needs no loading [2]. Despite these advantages, low melting metallic brazes limit the usage temperature of joint.

Transient liquid phase bonding, also named as isothermal solidification and diffusion brazing for joining at above 450 °C, facilitates the usage temperatures of joint to go above the joining temperature [3–6]. The trick of that is the total consumption of brazes and the simultaneous formation of high melting compounds between matrixes and brazes. This technique has been well proven applicable in joining some metallic and ceramic parts. Most brazes used are composed of metallic ingredients. Although the intermetallic compounds possess high melting points and high strength, their distinct electronic properties from ceramic bulk phases may lure corrosive aggression.

Recently, Chang and Huang published research on joining alumina (Al_2O_3) via a boron oxide (B_2O_3) interlayer and a joining strength above 150 MPa was achieved [7]. The success of joining Al_2O_3 via a B_2O_3 interlayer relies on the low eutectic temperature and on the presence of high melting compounds in the Al_2O_3–B_2O_3 phase diagram. Only a few binary ceramic systems possess a eutectic point below 1000 °C and a proper compound. Among them, the titanium dioxide (TiO_2) and bismuth oxide (Bi_2O_3) binary system is an ideal candidate system whose eutectic temperature is 835 °C and compounds melt at over 1200 °C. This data can be seen in Fig. 1, the Bi_2O_3–TiO_2 phase diagram [8]. TiO_2 is widely used as a catalyst in photoelectrochemical applications [9]; contrarily, little research has been done on the joining of TiO_2 [10]. In this paper, a study on the compound formation during the joining of TiO_2 bulk phases via a Bi_2O_3 interlayer by the transient liquid phase bonding technique is reported.

2. Experimental

99.9% TiO_2 powder (SHOWA, 2021-7760) and 99.9% Bi_2O_3 powder (ACROS, A102277101) were the raw materials.

---

* Corresponding author at: 250, Kuo-Kuang Road, Taichung, 40227, Taiwan, ROC. Tel.: +886 4 22840500x406; fax: +886 4 22852433.
E-mail address: lschang@dragon.nchu.edu.tw (L.S. Chang).

0272-8842/$36.00 © 2009 Elsevier Ltd and Techna Group S.r.l. All rights reserved.
doi:10.1016/j.ceramint.2009.03.001

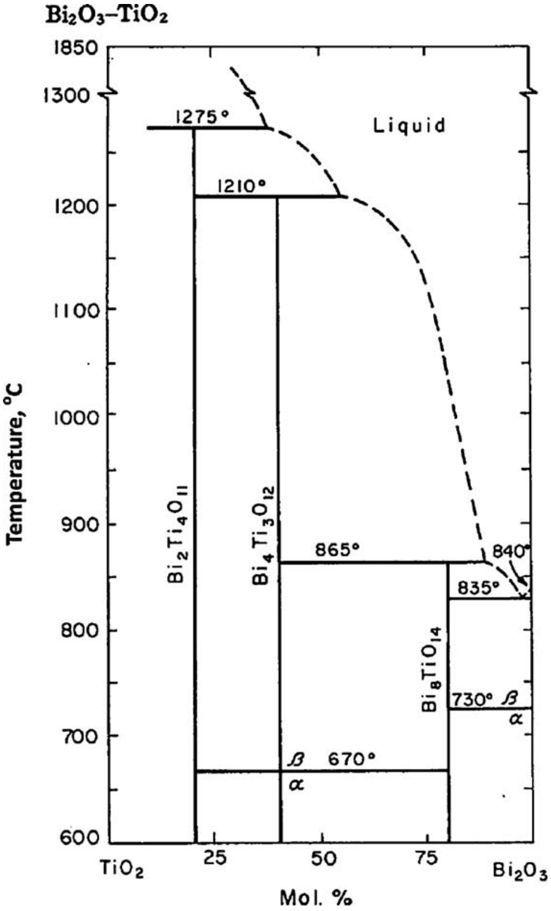

Fig. 1. Bi_2O_3–TiO_2 phase diagram [8].

Aqueous TiO_2 slurry with 50 wt. % solid content and 4 wt. % dispersant was prepared. The dispersant was Darvon 7. TiO_2 green cakes were formed by pressure slip casting of the slurry and then sintered at 1350 °C after dehydration at 40 and 60 °C for 1 day each, and de-dispersant at 200 °C for 6 h. The sintered bulks were cut into 2 cm × 1.5 cm × 1 cm pieces and polished. The density and crystal structures were measured by Archimedes' method and X-ray diffraction (XRD, MAC Science MXP3).

The Bi_2O_3 powder was mixed with a little water to get the ceramic paste. The paste was spread over one large side of the TiO_2 bulk with a 0.1 mm spacing blade process to form a Bi_2O_3 interlayer. An uncoated TiO_2 bulk was then put on the covered side of the TiO_2 bulk and a TiO_2–Bi_2O_3–TiO_2 sandwich was prepared. The sandwich samples were fastened with stainless steel wire and put into an electric furnace (Thermolyne, 1100). A small load of 1 kPa was applied on the samples to control the interlayer thickness at about 20 μm. The samples were pre-joined at 850 °C for 1.5 h. Then they were heated to three different temperatures (900, 1000, 1100 °C) and held for various times (0.5–72 h). Fig. 2 represents the schema of the materials evolution during the joining process.

The joined samples were cut, mounted, ground and polished in sequence. We observed the microstructure of the joint cross-section by scanning electron microscopy (SEM, JEOL JSM-5400) and analyzed the composition of the interface by electron probe microanalysis (EPMA, JEOL 8900R). The samples were also fractured to reveal the interlayer and the fractured surface was analyzed by XRD. The crystal structure and composition, respectively determined from XRD and EPMA, were mutually verified.

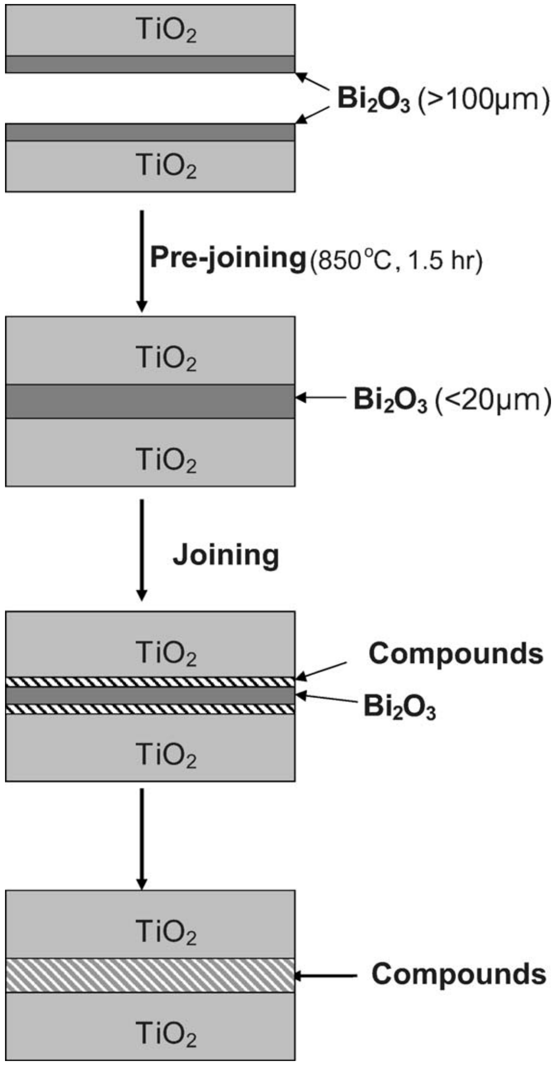

Fig. 2. Schema of materials evolution during the joining process.

3. Results and discussion

3.1. Compound formation in joints at various temperatures

The density of the TiO_2 bulk was 4.16 g/cm^3 (relative density: 98.3%). It is yellowish brown and has a rutile structure. Fig. 3 shows the SEM micrographs of the joint cross-sections in the samples heated at 900 °C for 0.5–24 h, where the dark area is TiO_2 and the cross-light area is the interlayer. Though polished, the sample surface is still scraggy due to the fragility of Bi_2O_3. After heated for 1 h, a 5 μm thick, light grey layer, labeled "A", arises at the B_2O_3–TiO_2 interface (Fig. 3a). The thickness of this layer increases with increased heating time. The light grey layer replaces the whole Bi_2O_3 interlayer after a 3 h heat treatment at 900 °C (Fig. 3b). The Ti/Bi ratio of the

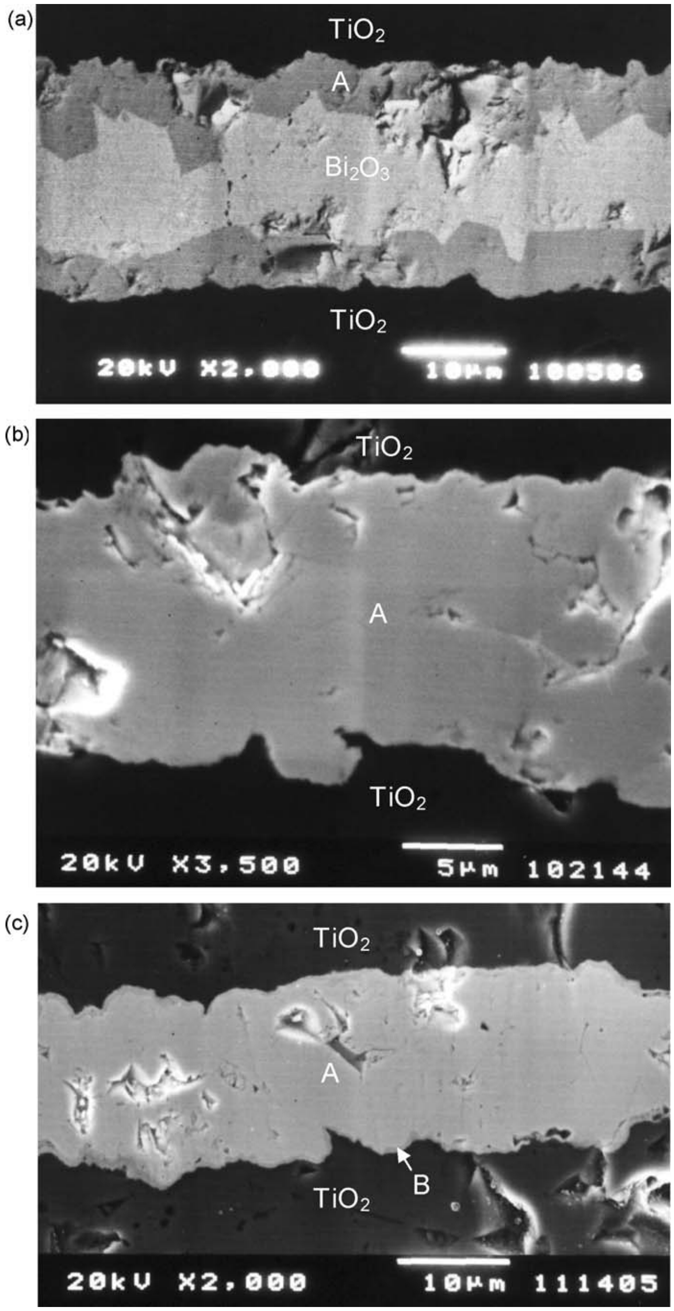

Fig. 3. SEM micrographs of the joint cross-sections heated at 900 °C for (a) 1 h, (b) 3 h and (c) 6 h.

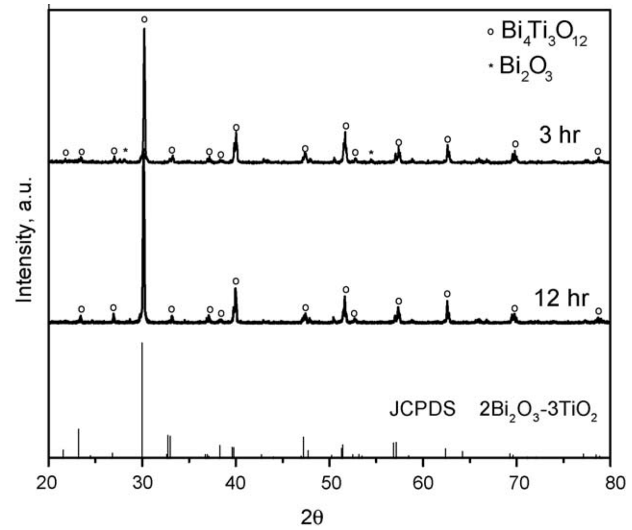

Fig. 4. XRD pattern of the fractured surface of the joint heated at 900 °C for 3 h.

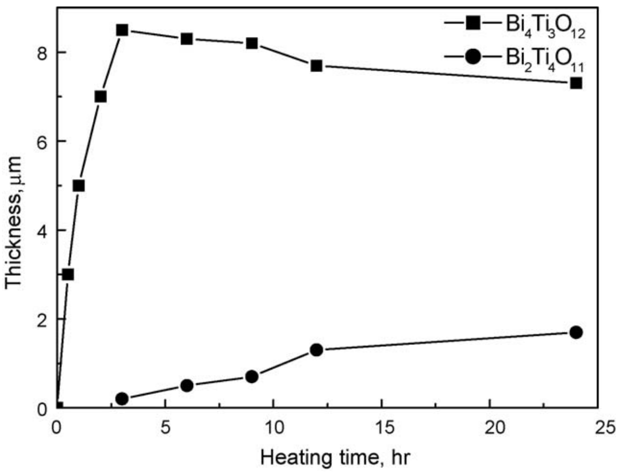

Fig. 5. Thickness of compounds in the joint region heated at 900 °C for various times.

compound A measured by EPMA is about 3/4 which corresponds to the $Bi_4Ti_3O_{12}$ compound. The XRD pattern of the fractured surface of this sample (Fig. 4) verifies that the compound A is $Bi_4Ti_3O_{12}$. The JCPDS (Joint Committee on Powder Diffraction Standards) spectrum of $Bi_4Ti_3O_{12}$ is also given at the bottom of Fig. 4 for comparison.

A darker compound (B) appears at the interface between TiO_2 and $Bi_4Ti_3O_{12}$ arising when the sample is heat treated for 6 h (Fig. 3c); its thickness is 0.5 µm and becomes thicker as heating goes on. It reaches 1.7 µm after a one-day long heat treatment at 900 °C. This compound B is $Bi_2Ti_4O_{11}$ according to the Bi/Ti = 2 from EPMA. The thicknesses of the interfacial compounds, $Bi_4Ti_3O_{12}$ and $Bi_2Ti_4O_{11}$, for various heating times are plotted in Fig. 5.

Heat treatments at 1000 °C for various times result in the formation of a three-layer structure of interfacial compounds. The SEM micrograph of the joint cross-section in the sample heated for 48 h is shown in Fig. 6a, for example. The three compounds are A: $Bi_4Ti_3O_{12}$, B: $Bi_2Ti_2O_7$ and C: $Bi_2Ti_4O_{11}$ as clearly indicated in Fig. 6b. It must be mentioned that the $Bi_2Ti_2O_7$ compound is in a metastable phase.

The thicknesses of these compounds are plotted in Fig. 7 as a function of heating time. $Bi_4Ti_3O_{12}$ initially forms and takes up the whole interlayer quite fast. Just after 0.5 h heating, no Bi_2O_3 is observed. $Bi_2Ti_4O_{11}$ arises at the interface between TiO_2 and $Bi_4Ti_3O_{12}$. It grows until the appearance of $Bi_2Ti_2O_7$. $Bi_2Ti_2O_7$ appears suddenly with a thickness of 2.5 µm in the sample heated for 6 h, and in the meantime $Bi_2Ti_4O_{11}$ tends to disappear abruptly. Thereafter both $Bi_2Ti_2O_7$ and $Bi_2Ti_4O_{11}$ grow steadily. The thickest $Bi_2Ti_2O_7$ is observed in the sample heated at 1000 °C for 24 h, while $Bi_4Ti_3O_{12}$ reaches its

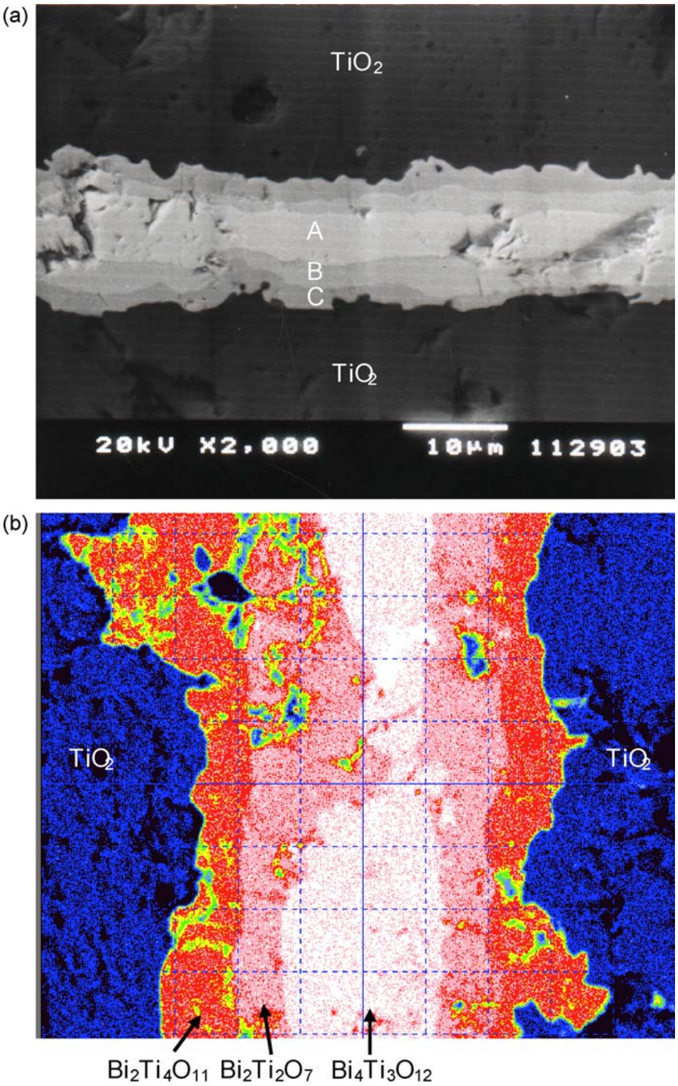

Fig. 6. Joint cross-section in the sample heated for 48 h: (a) the SEM micrograph and (b) chemical mapping from EPMA.

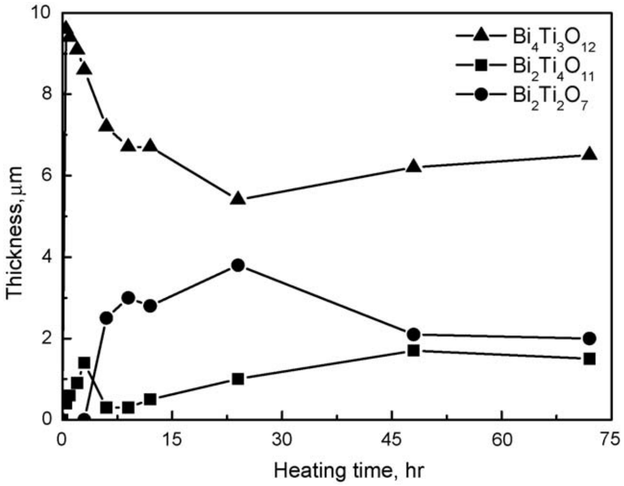

Fig. 7. Thickness of compounds in the joint region heated at 1000 °C for various times.

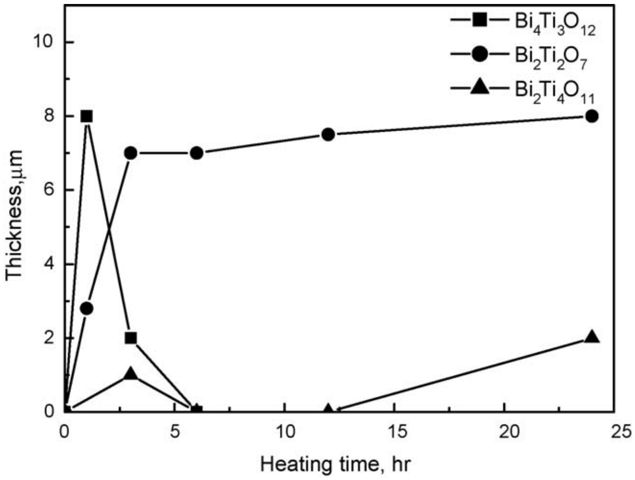

Fig. 8. Thickness of compounds in the joint region heated at 1100 °C for various times.

maximum thickness. After a 48 h or longer heat treatment, the thicknesses of these three compounds do not change any more.

Fig. 8 represents the thickness of compounds vs. heating time diagram at 1100 °C. As the joining temperature increases close to the incongruent melting point 1210 °C of $Bi_4Ti_3O_{12}$, $Bi_4Ti_3O_{12}$ appears and vanishes from the interlayer within 6 h. After that, the metastable $Bi_2Ti_2O_7$ phase is the dominant one. $Bi_2Ti_4O_{11}$ is found in the 3 h sample, but in samples heated for longer times it remains undetectable until the sample is heated for 24 h.

Fig. 9 shows the SEM micrograph of the joint cross-section heated at 1100 °C for 24 h. As mentioned previously, the dominant light grey phase (A) is $Bi_2Ti_2O_7$ and the darker stripe (B) at its fringes is $Bi_2Ti_4O_{11}$. The holes in the middle of the interlayer ($Bi_2Ti_2O_7$) may result from the formation of the stable $Bi_2Ti_4O_{11}$ phase. The diffusion of Bi atoms from $Bi_2Ti_2O_7$ (source) toward the $Bi_2Ti_4O_{11}$ (sink) leaves vacancies behind. The holes are the aggregations of these vacancies which are quite mobile at this elevated temperature. The holes may give rise to a severe embrittlement of the joint.

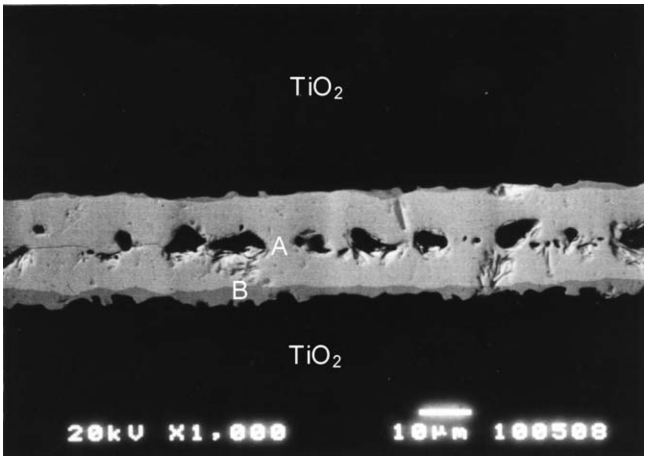

Fig. 9. SEM micrograph of the joint cross-section heated at 1100 °C for 24 h.

3.2. Activation energy of compound formation

The equation $x = (Kt)^n$ is the typical equation to describe the growth kinetics of an interfacial compound, where x is the compound thickness, K is the growth constant, t is time and n is the characteristic growth exponent. In the case of a diffusion-controlled growth, $n = 0.5$. If $n = 1$, the interfacial reaction is the dominant path for growth. Fig. 10 represents three thickness-time diagrams in a log scale for $Bi_4Ti_3O_{12}$, $Bi_2Ti_4O_{11}$ and $Bi_2Ti_2O_7$, respectively. The data for compound thickness in a three-layer growth was not taken into consideration. The corresponding slopes are 0.57, 0.68 and 0.28 for these compounds. The fact that the growth of $Bi_4Ti_3O_{12}$ and $Bi_2Ti_4O_{11}$ is apparently diffusion-controlled can be seen, while that of $Bi_2Ti_2O_7$ is undetermined probably due to the data scattering.

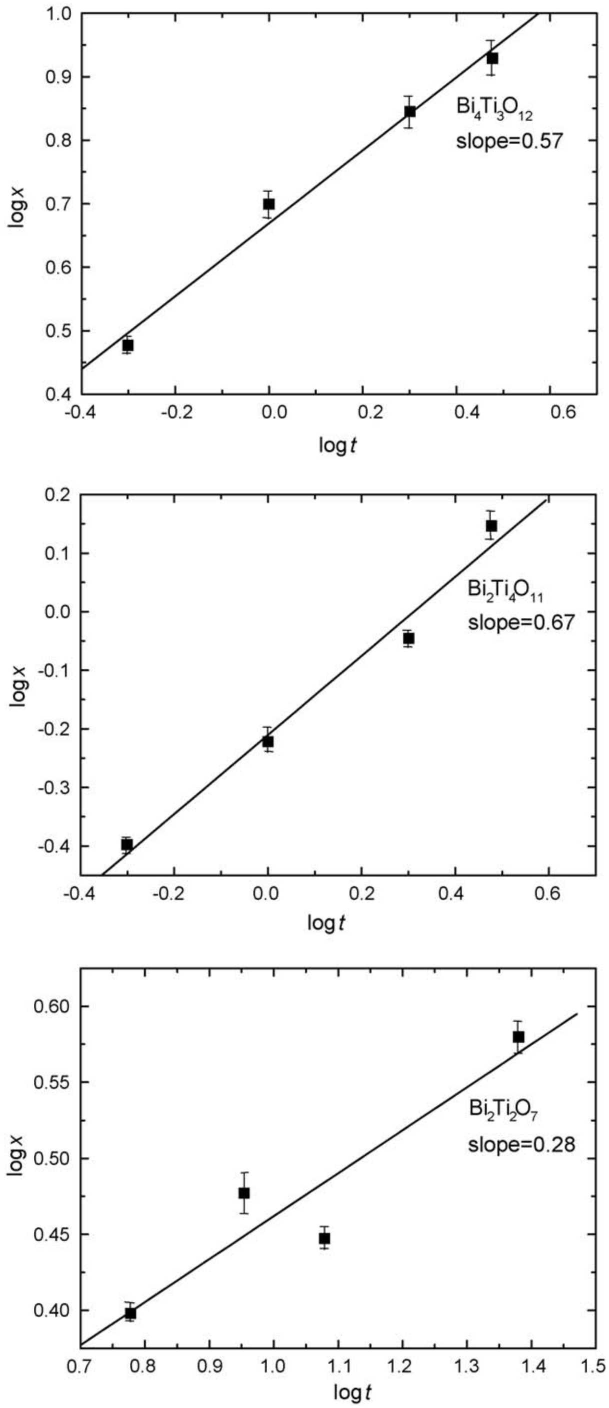

Fig. 10. Thickness-time diagrams in a log scale for three compounds.

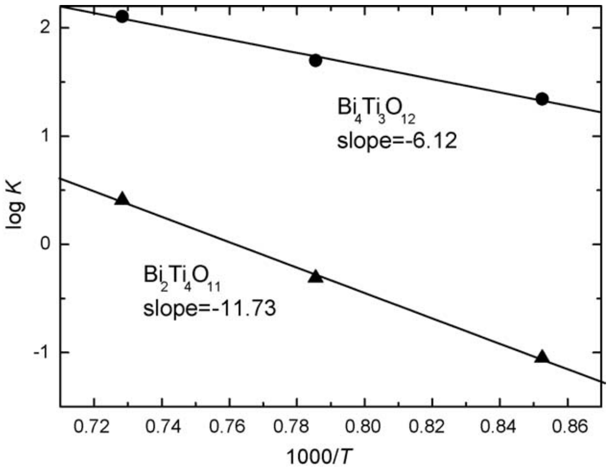

Fig. 11. log K–1000/T diagram for two compounds.

The growth constant K for $Bi_4Ti_3O_{12}$ and $Bi_2Ti_4O_{11}$ at 900, 1000 and 1100 °C has been calculated, and, according to the Arrhenius relationship, determined the activation energies of growth from the log K–1000/T diagram (Fig. 11) as

$$Q(\mathrm{Bi_4Ti_3O_{12}}) = 50\,\mathrm{kJ/mol}$$

$$Q(\mathrm{Bi_2Ti_4O_{11}}) = 98\,\mathrm{kJ/mol}$$

$Bi_4Ti_3O_{12}$ has lower activation energy of growth and forms first at the interface between TiO_2 and Bi_2O_3.

4. Conclusion

The growth of interfacial compounds between TiO_2 and Bi_2O_3 during transient liquid phase bonding at various temperatures for various times was investigated in this study. The microstructures and compositions of compounds in joints were analyzed by means of SEM and EPMA. The crystal structures of some compounds were verified by XRD. It can be concluded that in the samples heated at 900, 1000 and 1100 °C, the compound $Bi_4Ti_3O_{12}$ forms initially and replaces the Bi_2O_3 interlayer. $Bi_2Ti_4O_{11}$ arises secondly at the interface between $Bi_4Ti_3O_{12}$ and TiO_2 and the metastable $Bi_2Ti_2O_7$ phase appears last at the interface between $Bi_4Ti_3O_{12}$ and $Bi_2Ti_4O_{11}$. The growth of $Bi_4Ti_3O_{12}$ and $Bi_2Ti_4O_{11}$ is diffusion-controlled with activation energies of 50 and 98 kJ/mol, respectively. Holes in the middle of the joint heated at 1100 °C for 24 h were also found. These holes are probably the aggregates of vacancies which may be induced from the diffusion of Bi atoms accompanying the formation of $Bi_2Ti_4O_{11}$.

Acknowledgement

The authors would like to thank National Science Council of the Republic of China for its financial support under Contract No. NSC90-2216-E-005-021.

References

[1] O.M. Akselsen, Diffusion bonding of ceramics, J. Mater. Sci. 27 (3) (1992) 569–579.

[2] O.M. Akselsen, Advances in brazing of ceramics, J. Mater. Sci. 27 (3) (1992) 1989–2000.

[3] A.M. Glaeser, The use of transient FGM interlayers for joining advanced ceramics, Composites Part B: Eng. 28B (1–2) (1997) 71–84.

[4] W.F. Gale, Transient liquid phase bonding of intermetallic compounds, Mater. Sci. Forum 426–432 (3) (2003) 1891–1896.

[5] M.R. Locatelli, B.J. Dalgleish, K. Nakahima, A.P. Tomsia, A.M. Glaeser, New approaches to joining ceramics for high-temperature applications, Ceram. Int. 23 (4) (1997) 313–322.

[6] S.D. Peteves, M. Paulasto, G. Ceccone, V. Stamos, Reactive route to ceramic joining: fabrication, interfacial chemistry and joint properties, Acta Mater. 46 (7) (1998) 2407–2414.

[7] L.-S. Chang, C.-F. Huang, Transient liquid phase bonding of alumina to alumina via boron oxide interlayer, Ceram. Int. 30 (8) (2004) 2121–2127.

[8] E.M. Levin, C.R. Robbins, H.F. McMurdie, Phase Diagrams for Ceramists, vol. II, The American Ceramic Society, 1969, p. 99, Fig. 2360.

[9] P. Fernández-Ibáñez, F.J. de las Nieves, S. Malato, Titanium dioxide/electrolyte solution interface: electron transfer phenomena, J. Colloid Interface Sci. 227 (2) (2000) 510–516.

[10] L. Sudheendra, M.K. Renganathan, A.R. Raju, Bonding of monazite to Al_2O_3 and TiO_2 ceramics, Mater. Sci. Eng. A 281 (1) (2000) 259–262.